Molecular Structure−Property Relationships for Electron-Transfer Rate Attenuation in Redox-Active Core Dendrimers

Christopher B. Gorman,* Jennifer C. Smith, Michael W. Hager, Brandon L. Parkhurst, Hanna Sierzputowska-Gracz, and Carol A. Haney

Contribution from the Department of Chemistry, North Carolina State University, Box 8204, Raleigh, North Carolina 27695-8204

Received March 18, 1999. Revised Manuscript Received September 3, 1999

Abstract: Two series of redox-active, iron−sulfur core dendrimers of the general structure $(nBu_4N)_2[Fe_4S_4$-$(S\text{-Dend})_4]$ (Dend = dendrons of generations 1 through 4) were prepared. Heterogeneous electron-transfer rate constants indicated that the rigid series of dendrimers were more effective at attenuating the rate of electron transfer than were the flexible series of dendrimers. These results were rationalized using computationally derived models which indicated an offset and mobile iron−sulfur core in the flexible series of molecules and a more central and relatively immobile iron−sulfur core in the rigid series of molecules. Further consideration of these data indicated that, while the dendrimers containing rigid ligands had better encapsulated redox cores for a given molecular weight, these molecules had higher electron-transfer rates for a given molecular radius.

Introduction

Control of electron-transfer kinetics is a central theme in biology and is a rapidly emerging concern in the new field of nanoscale electronics. Electron-transfer proteins have evolved to control precisely the rate of electron transfer from one redox center to another. Gray et al. dramatically illustrated that the relative rate of electron transfer from a redox center to various points at the surface of heme-based proteins can vary substantially.[1−3] How are electron-transfer rates to/from a redox center governed by a "nonconducting", encapsulating molecular shell?[4−7] Understanding how electron transfer is governed by a topologically regular architecture of a given size would help explain how the structural features in the specific but topologically complex electron-transfer proteins govern electron-transfer rates.

In addition, the notion of encapsulation is anticipated to be of critical importance in isolation of information in as yet unprecedented single-molecule information storage schemes. In such a scheme, the presence or absence of single electrons on individual molecules encode binary information. This scheme would represent the smallest possible switch and nominally the way to implement the highest density memory.[8,9] To a chemist, this idea translates very naturally into the notion of an array of oxidized and reduced molecules. Placing oxidized molecules in close proximity to reduced molecules to create this ordered array invites rapid electron transfer between the "0"s and "1"s, scrambling information. Thus, molecular structure−property relationships that govern the rate of electron transfer between redox centers will be required to implement a one electron = one bit information storage scheme in a rational way.

We have prepared and studied redox active, metal cluster core dendrimers to affect the relative rate of electron transfer to/from encapsulated centers.[10−13] These dendrimers represent topologically well-defined architectures designed to isolate the redox state of the core − effectively attenuating the rate of electron transfer to/from the molecular center to some degree. Metallodendrimers have had substantial recent study as functional, supramolecular objects. Particularly relevant to the idea of encapsulation is the observation of shifts in the electronic absorption maxima,[14,15] fluorescence efficiency,[16,17] and redox potentials[18] of porphyrin core dendrimers as well as attenuation of their reaction with dioxygen.[19,20]

In this paper, we characterize quantitatively the size and heterogeneous electron-transfer rate attenuation of the iron−sulfur core dendrimers previously reported. Moreover, we report

(1) Langen, R.; Chang, I. J.; Germanas, J. P.; Richards, J. H.; Winkler, J. R.; Gray, H. B. *Science* **1995**, *268*, 1733−1735.

(2) Wuttke, D. S.; Bjerrum, M. J.; Winkler, J. R.; Gray, H. B. *Science* **1992**, *256*, 1007−1009.

(3) Winkler, J. R.; Gray, H. B. *Chem. Rev.* **1992**, *92*, 369−379.

(4) Beratan, D. N.; Onuchic, J. N.; Winkler, J. R.; Gray, H. B. *Science* **1992**, *258*, 1740−1741.

(5) Skourtis, S. S.; Beratan, D. N. *J. Phys. Chem. B* **1997**, *101*, 1215−1234.

(6) Risser, S. M.; Beratan, D. N.; Onuchic, J. N. *J. Phys. Chem.* **1993**, *97*, 4523−4527.

(7) Beratan, D. N.; Skourtis, S. S. *Curr. Opin. Chem. Biol.* **1998**, *2*, 234−243.

(8) Gorman, C. B. *Adv. Mater.* **1997**, *9*, 1117−1119.

(9) This statement assumes computing based on conventional on-state/off-state processing. Conceivably, more than one bit of information could be stored by an electron using quantum computing schemes (qubits). However, such arguments extend beyond what is purported here.

(10) Chen, K.-Y.; Gorman, C. B. *J. Org. Chem.* **1996**, *61*, 9229−9235.

(11) Gorman, C. B.; Parkhurst, B. L.; Chen, K.-Y.; Su, W. Y. *J. Am. Chem. Soc.* **1997**, *119*, 1141−1142.

(12) Gorman, C. B.; Hager, M. W.; Parkhurst, B. L.; Smith, J. C. *Macromolecules* **1998**, *31*, 815−822.

(13) Gorman, C. B.; Miller, R. L.; Chen, K.-Y.; Bishop, A. R.; Haasch, R. T.; Nuzzo, R. G. *Langmuir* **1998**, *14*, 3312−3319.

(14) Dandliker, P. J.; Diederich, F.; Gisselbrecht, J.-P.; Louati, A.; Gross, M. *Angew. Chem., Int. Ed. Engl.* **1995**, *34*, 2725−2728.

(15) Tomoyose, Y.; Jiang, D.-L.; Jin, R.-H.; Aida, T.; Yamashita, T.; Horie, K.; Yashima, E.; Okamoto, Y. *Macromolecules* **1996**, *29*, 5236−5238.
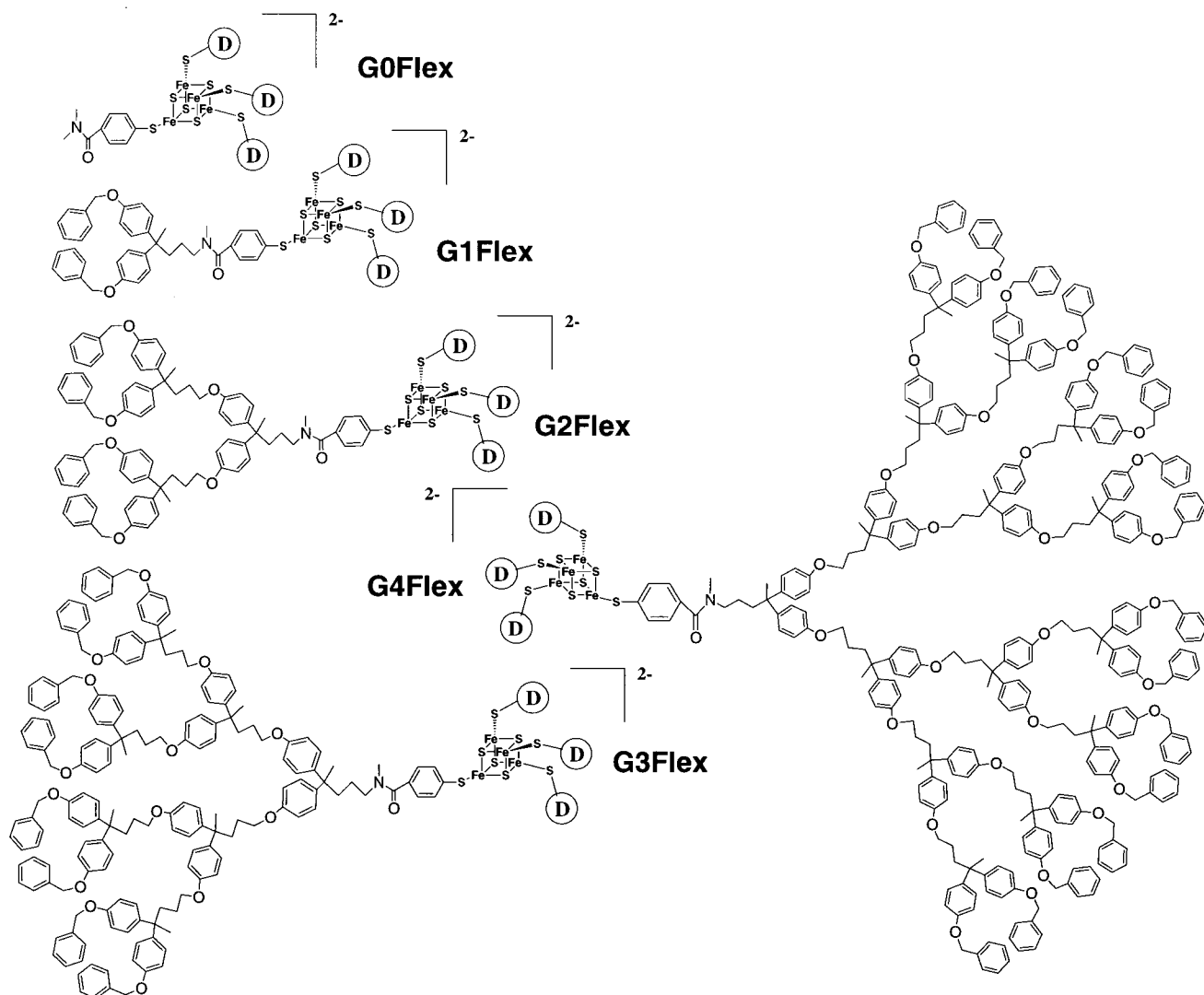
(16) Jin, R. H.; Aida, T.; Inoue, S. *Chem. Commun.* **1993**, 1261−1263.

(17) Sadamoto, R.; Tomioka, N.; Aida, T. *J. Am. Chem. Soc.* **1996**, *118*, 3978−3979.

(18) Dandliker, P. J.; Diederich, F.; Gross, M.; Knobler, C. B.; Louati, A.; Sanford, E. M. *Angew. Chem., Int. Ed. Engl.* **1994**, *33*, 1739−1741.

(19) Collman, J. P.; Fu, L.; Zingg, A.; Diederich, F. *Chem. Commun.* **1997**, 193−194.

(20) Jiang, D.-L.; Aida, T. *Chem. Commun.* **1996**, 1523−1524.

Figure 1. Flexible dendrimers considered in this study. One arm of each structure is drawn out fully. The three other arms are identical with the one shown but are abbreviated as a circled-D for ease of visualization.

the synthesis and characterization of a new class of iron−sulfur core dendrimers based on stiff, phenylacetylene-type linkages. It will be shown that ligand structure has an important effect on electron transfer rate attenuation in these redox-core dendrimers and that this effect is likely due to the conformation that the dendrimer molecules adopt.

Results and Discussion

A. "Flexible" Iron−Sulfur Core Dendrimers. We have previously reported the synthesis and preliminary electrochemical characterization of a series of globular iron−sulfur core dendrimers based on a relatively flexible repeat unit (Figure 1).[11,12] Previously the molecular weights of these molecules had been characterized only by vapor phase osmometry. In this work, the molecular weights were confirmed by either electrospray ionization mass spectrometry (ESI-MS) or matrix-assisted laser desorption ionization mass spectrometry (MALDI-MS).

B. "Rigid" Iron−Sulfur Core Dendrimers. To compare with the flexible iron−sulfur core dendrimers discussed above, a series of iron−sulfur core dendrimers were prepared that consisted of rigid phenyl acetylene-type ligands (Figure 2). The naming convention adopted here was chosen so that flexible and rigid molecules of the same generation have similar molecular weights. Dendrimers composed of this repeat unit

had previously been reported by Moore et al.[21,22] The synthesis of these molecules began with a series of focally substituted aromatic iodide dendrons also reported by Moore et al.[21,22] This chemistry worked well in our hands and was accomplished with only slight modifications discussed in the Experimental Section. An aromatic thiol focal point was constructed by preparing *p*-ethynyl benzene thioacetate and this was reacted with the focally substituted aromatic iodide dendrons of generations 0 through 4 (Scheme 1).

Initially, it was our intention to deprotect the thioacetate group from each of these molecules and react them with the iron−sulfur cluster. Indeed this chemistry was successful to form **G0Rigid** (Figure 2). However, for reasons that are unclear, the larger dendrons rapidly reacted to form the symmetric disulfide even when precautions were taken to avoid oxygen during the deprotection.[23] It was found, however, that the deprotection and subsequent ligand exchange could be carried out in one pot to form the series of rigid iron−sulfur core dendrimers. As before,[11]

(21) Xu, Z.; Kahr, M.; Walker, K. L.; Wilkins, C. L.; Moore, J. S. *J. Am. Chem. Soc.* **1994**, *116*, 4537−4550.

(22) Bharathi, P.; Patel, U.; Kawaguchi, T.; Pesak, D. J.; Moore, J. S. *Macromolecules* **1995**, *28*, 5955−5963.

(23) This problem and the general strategy of in situ deprotection has been described: Tour, J. M.; Jones, L., II; Pearson, D. L.; Lamba, J. J. S.; Burgin, T. P.; Whitesides, G. M.; Allara, D. L.; Parikh, A. N.; Atre, S. V. *J. Am. Chem. Soc.* **1995**, *117*, 9529−9534.
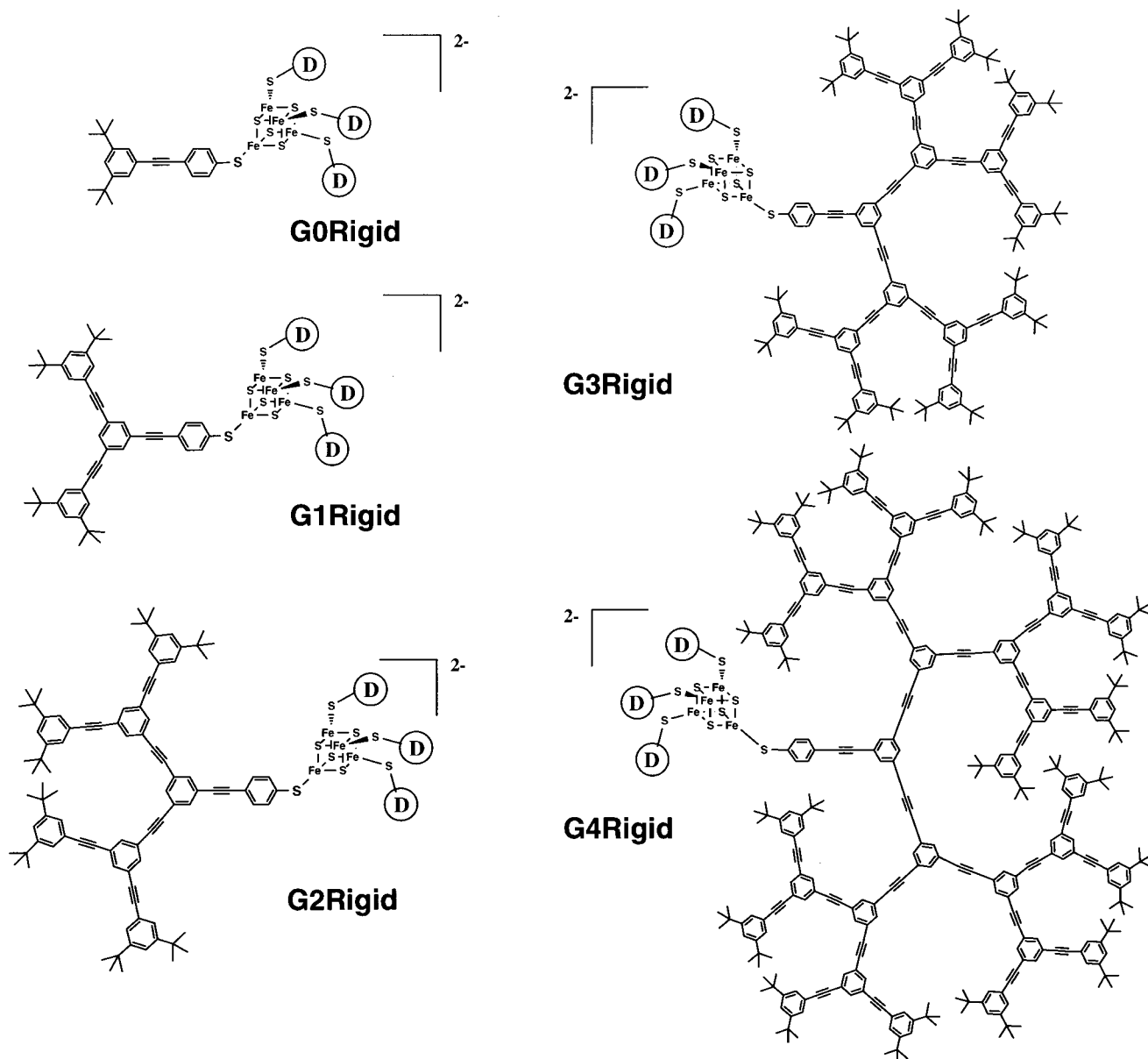
Figure 2. Rigid dendrimers prepared and considered in this study. One arm of each structure is drawn out fully. The three other arms are identical with the one shown but are abbreviated as a circled-D for ease of visualization.

Scheme 1
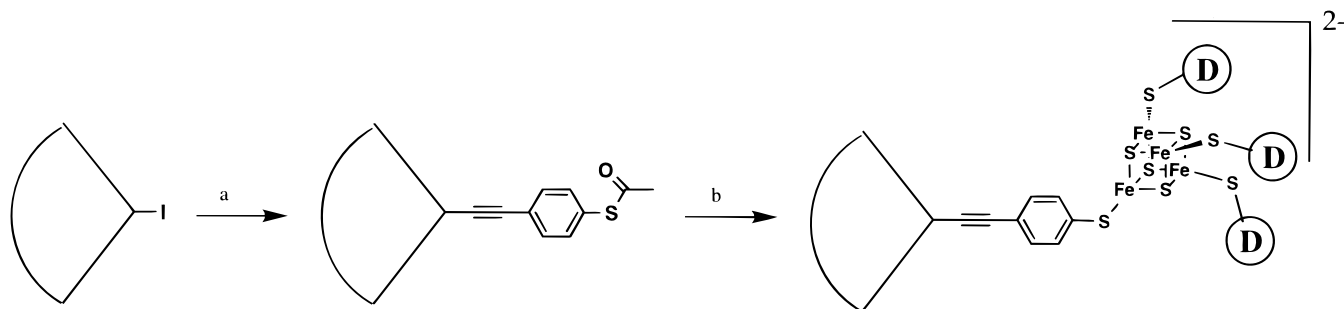
a (4-Ethynyl) phenyl thioacetate, Pd$_2$(dba)$_3$, CuI, PPh$_3$, *i*PrEt$_2$N, THF, 65 °C. *b* (1) NH$_4$OH, 1 h, room temperature; (2) (nBu$_4$N)$_2$[Fe$_4$S$_4$(S*t*Bu)$_4$], DMF, 40 °C.

ligand exchange[24] proceeded smoothly in dimethylformamide solution with slight heating and application of dynamic vacuum to remove the *tert*-butyl thiol reaction byproduct.

(24) Que, L., Jr.; Bobrik, M. A.; Ibers, J. A.; Holm, R. H. *J. Am. Chem. Soc.* **1974**, *96*, 4168−4177.

C. Determination of Diffusion Coefficients. Diffusion coefficients of these dendrimers in dilute solution were determined using two complementary methods: by pulsed field gradient spin−echo proton NMR (PFGSE-^{1}H NMR) and electrochemically by chronoamperometry (Table 1). With these

Table 1. Diffusion Coefficients, D_o (cm^2/s) Obtained from Pulsed Field Gradient Spin−Echo NMR Spectroscopy (PFGSE) and Chronoamperometry (CA) and Corresponding Stokes−Einstein Radius, R_H

structure	D_o ($\times 10^6$ cm^2/s) PFGSE 1 mM DMF[a]	R_H (Å) DMF[a,b]	D_o ($\times 10^6$ cm^2/s) PFGSE 0.1 mM THF[a]	R_H (Å) THF[a,b]	D_o ($\times 10^6$ cm^2/s) CA 1 mM DMF[a]	R_H (Å) DMF[a,b]	molecular model R_g (Å)[e]
G1Flex	3.10(0.07)	8.80(0.11)	3.76(0.20)	12.63(0.61)	3.47(0.16)	7.85(0.37)	7.75
G2Flex	2.06(0.22)	13.22(0.91)	2.83(0.20)	16.76(1.09)	2.51(0.38)	10.86(1.94)	10.84
G3Flex	1.69(0.20)	16.04(1.23)	1.86(0.48)	25.48(5.22)	2.02(0.49)	13.49(4.02)	13.07
G4Flex	1.37(0.38)	19.93(3.99)	1.33(0.08)	35.80(0.10)	—[c]	—[c]	16.92
G1Rigid	2.72(0.12)	10.04(0.23)	4.84(0.09)	9.81(0.18)	2.17(0.46)	12.56(3.36)	15.02
G2Rigid	2.11(0.05)	12.92(0.19)	3.88(0.40)	12.22(1.13)	1.89(0.37)	14.43(3.50)	18.70
G3Rigid	—[d]	—[d]	3.28(0.58)	14.46(2.16)	—[d]	—[d]	20.89
G4Rigid	—[d]	—[d]	3.01(0.22)	15.78(1.09)	—[d]	—[d]	24.84

[a] Values in parentheses represent the magnitude of the 90% confidence intervals of these values. [b] Calculated from eq 2. [c] Irreversible electrochemistry prevented this value from being determined. [d] Insufficiently soluble. [e] Average of all structures within a Boltzmann cutoff (10 kcal/mol @ 500 K) of the lowest energy structure found in the conformational search.

values in hand, electrochemistry was used to determine heterogeneous electron-transfer rate constants (Section D). Also, these values in combination with an appropriate model provided an indication of molecular size. This estimated size was correlated with modeling results (Section E).

PFGSE-NMR had been used previously by Newkome and Johnson[25,26] and Ihre et al.[27] to determine diffusion coefficients and hydrodynamic radii of dendrimers. For noninteracting objects diffusing in a medium of viscosity η, the hydrodynamic radius is given by the Stokes−Einstein equation

$$R_H = k_b T / 6 \pi \eta D \qquad (1)$$

Ihre et al. found a good correlation between measured and estimated radii for such dendrimers assuming a hard-sphere model. We found such correlations to be very solvent and molecule dependent as discussed further below.

To our knowledge, quantitative electrochemical techniques have been used only in one example to obtain diffusion information for redox-active dendrimers. In this case, Cardona and Kaifer[28] used a digital simulation of cyclic voltammetric data to obtain this value, the heterogeneous electron-transfer rate constant (k), and the transfer coefficient (α). We chose to use chronoamperometry as this technique requires a diffusion coefficient as the only free parameter in a fit of these data.

Several trends were noted in the data shown in Table 1. As would be expected, a decrease in diffusion coefficient was found with increasing molecular size within a given series of molecules. In comparing the flexible series with the rigid series of metallodendrimers, the most notable contrast in diffusion behavior was observed as solvent was varied. As THF and DMF have different viscosities, diffusion coefficients determined in these two solvents are not comparable. Thus, hydrodynamic radii were calculated using eq 1 above and these were compared.

The flexible series of dendrimers displayed a large change in hydrodynamic radius in different solvents. Specifically, these molecules appeared much larger in THF than in DMF, probably due to greater "solvent swelling" in the former solvent compared with the latter. Note that the data obtained in THF were at a 10-fold lower concentration than those obtained in DMF. Initially, we were concerned about comparing these two sets of data because of this difference. However, these solutions

should all be dilute enough that intermolecular interactions are negligible. However, if concentration were an issue, a decrease in intermolecular interactions in the more dilute THF solutions would result in an increase in the apparent diffusion coefficient. This supposed increase in apparent diffusion coefficient would decrease the apparent hydrodynamic radius calculated. However, the hydrodynamic radii in THF were found to be greater than those in DMF. Thus any concentration effect is not a concern. The data obtained by chronoamperometry suggest a further decrease in hydrodynamic radius in DMF/electrolyte solution compared to the neat DMF solution used for the PFGSE experiments. The increase in ionic strength alone will make the solution slightly more viscous. This viscosity increase would increase the apparent hydrodynamic radius as per eq 1. However, since the opposite was observed, these data suggest that these molecules further contract in DMF solution containing electrolyte. This postulated size difference may be a factor in the difference in effective reduction/oxidation kinetics of these molecules in different solvents (Section D).

In contrast to the above results, the rigid dendrimers showed little change in computed hydrodynamic radius as a function of solvent. This observation indicates that these molecules do not change substantially in size or shape, consistent with the rigid and thus "shape persistent"[29−31] nature of these molecules.

When considering the flexible dendrimers in the most compact form studied (i.e., in DMF/electrolyte), the computed hydrodynamic radii of the these molecules correlated well with the radii of gyration calculated using molecular dynamics simulations (Section E). This correlation should exist only if these molecules were behaving as hard spheres in which the interaction with solvent was minimal. In contrast, the rigid dendrimers did not exhibit this correlation, suggesting a nonspherical/noncompact shape for these molecules. Shape rather than degree of solvation is suggested to be most important in interpreting the diffusion data for the rigid dendrimers as little change in molecular size was observed above in different solvents. These conclusions also will be shown to be consistent with simulations described below.

D. Determination of Heterogeneous Electron-Transfer Rate Constants. The general question as to how macromolecular architectures quantitatively affect electron transfer to/ from incorporated redox species[32] has not been probed in detail. As described above, the quantitative electrochemical behavior of dendrons containing focal, redox-active (ferrocenyl)

(25) Newkome, G. R.; Young, J. K.; Baker, G. R.; Potter, R. L.; Audoly, L.; Cooper, D.; Weis, C. D.; Morris, K.; Johnson, C. S, Jr. *Macromolecules* **1993**, *26*, 2394−2396.

(26) Young, J. K.; Baker, G. R.; Newkome, G. R.; Morris, K. F.; Johnson, C. S., Jr. *Macromolecules* **1994**, *27*, 3464−3471.

(27) Ihre, H.; Hult, A.; Söderlind, E. *J. Am. Chem. Soc.* **1996**, *118*, 6388−6395.

(28) Cardona, C. M.; Kaifer, A. E. *J. Am. Chem. Soc.* **1998**, *120*, 4023−4024.

(29) Moore, J. S. *Acc. Chem. Res.* **1997**, *30*, 402−413.

(30) Morgenroth, F.; Reuther, E.; Müllen, K. *Angew. Chem., Int. Ed. Engl.* **1997**, *36*, 631−634.

(31) Morgenroth, F.; Kübel, C.; Müllen, K. *J. Mater. Chem.* **1997**, *7*, 1207−1211.

(32) Gorman, C. B. *Adv. Mater.* **1998**, *10*, 295−309.

Table 2. Heterogeneous Electron-Transfer Rate Constant (k_0), Reduction Potential ($E_{1/2}$), and α for the One-Electron Redox Couple $[Fe_4S_4(S\text{-Dend})_4]^{2-/3-}$

	CV[a]		OSWV[a]		
structure	k_0 (×10³) cm/s	$E_{1/2}$ (mV)	k_0 (×10³) cm/s	$E_{1/2}$ (mV)	α OSWV[a]
G0Flex	8.63(0.83)	−1352(3)	7.43(1.31)	−1344(4)	0.57(0.07)
G1Flex	8.36(0.89)	−1360(6)	6.15(0.64)	−1359(9)	0.54(0.06)
G2Flex	3.59(0.33)	−1366(10)	3.29(0.44)	−1374(13)	0.33(0.01)
G3Flex	0.51(0.22)	−1371(19)	0.76(0.03)	−1374(28)	0.29(0.05)
G4Flex	irreversible	irreversible	0.13(0.06)	N. A.[b]	0.47(0.01)
G0Rigid	8.95(0.96)	−1354(4)	6.24(0.59)	−1351(5)	0.56(0.08)
G1Rigid	5.13(1.11)	−1323(16)	4.12(0.78)	−1322(14)	0.54(0.04)
G2Rigid	2.13(0.36)	−1329(13)	2.35(0.09)	−1324(9)	0.37(0.03)

[a] The magnitude of the 90% confidence interval is indicated in parentheses. [b] Not determined in a fit of an irreversible wave.

groups has been described.[28] Several redox-active porphyrin−core and metal tris-bipyridine−core dendrimers have been prepared and their redox potentials determined by cyclic voltammetry,[14−20,28,32−40] but no quantitative electrochemistry experiments have been reported on these molecules to our knowledge.

To probe how the electron-transfer rate of the redox-active core is affected by various dendritic architectures, heterogeneous electron-transfer rate constants (k_0) were determined for these molecules. These determinations were made in two ways: (1) via a Nicholson analysis of the cyclic voltammograms (CVs) of these molecules taken at a number of scan rates and (2) by an iterative fit of their Osteryoung square wave voltammograms (OSWV) (see Experimental Section for details). The results of these experiments are shown in Table 2.

Cyclic voltammetry provided an indication as to whether electron-transfer rates were measured under the condition that the species was behaving as a freely diffusing redox probe. The kinetic analyses used here assume this behavior. Dendrimer adsorption to electrodes has been observed previously[41] and is thus a concern when macromolecular electrochemistry is performed. Plots of peak reductive current (from cyclic voltammetry) versus the square root of scan rate should be linear if the redox probe is freely diffusing. Indeed (see Supporting Information) this behavior is observed for the flexible dendrimers and in rigid dendrimers up to the second generation. However, with the molecule **G3Rigid**, a substantial deviation from linearity was observed. This molecule was also observed to be much less soluble in DMF. The molecule **G4Rigid** was so insoluble in DMF that cyclic voltammetry results could not be obtained. Thus, due to this experimental limitation, quantitative determination of electron-transfer rate constants of these larger rigid dendrimers was prohibited.

In a mixture of 25% pyridine and 75% DMF (v/v), the molecule **G3Rigid** was soluble enough for electrochemistry and

Figure 3. CVs taken in 25% pyridine/75% DMF (v/v) at a scan rate of 2 mV/s illustrating irreversible electron transfer for **G3Rigid** but still quasireversible electron transfer for **G3Flex**.

could be compared to **G3Flex**. The results of cyclic voltammetry (Figure 3) indicate that although **G3Flex** displays quasireversible behavior, the behavior of **G3Rigid** is irreversible. This result indicates that electron transfer is at least an order of magnitude slower for **G3Rigid** than for **G3Flex** under these conditions. Rate constants were not calculated in these cases due to concerns about error associated with uncompensated solution resistance in this lower dielectric solvent system.

The most confident measurements of electron-transfer rates came from Osteryoung square wave voltammograms (see Supporting Information). These data were fit to obtain the data shown in Table 2. The behavior of **G4Flex** was fit to an irreversible model to obtain a rate constant.[42] The position of the current maximum moves from molecule to molecule and for **G4Flex,** it shifts substantially. This behavior is expected due to a change in electron-transfer rate and does not reflect a large change in the thermodynamic redox potential.[42]

The change in thermodynamic redox potential in this series of molecules was, if anything, small. This result was initially surprising as investigations on porphyrin−core dendrimers concluded that a dendritic architecture could result in a large change in redox potential.[18] The redox potential of iron−sulfur clusters is rather sensitive to environmental changes.[43−45] This result suggests that these particular dendrimers attenuate electron transfer without substantially changing the local environment in which the redox species resides. This idea will be probed more below.

Several interesting changes were observed in electron-transfer rate both as molecules of different molecular weight and as the rigid and flexible molecules were compared. Figure 4 graphically illustrates the attenuation in heterogeneous electron-transfer rate as a function of molecular size and type. Since the two series of molecules are dissimilar in structure, molecular weight was chosen as the variable by which to compare them. Arguably, this parameter is most significant from the standpoint of molecular design as it represents a scale of synthetic effort. Although fewer data are available to assess quantitatively the attenuation in the rigid series of dendrimers, the rigid molecules clearly have lower electron-transfer rates than the flexible molecules for a given molecular weight. Clearly, there is an architectural difference that is important in governing this

(33) Bhyrappa, P.; Young, J. K.; Moore, J. S.; Suslick, K. S. *J. Am. Chem. Soc.* **1996**, *118*, 5708−5711.

(34) Tomioka, N.; Takasu, D.; Takahashi, T.; Aida, T. *Angew. Chem., Int. Ed. Engl.* **1998**, *37*, 1531−1534.

(35) Norsten, T.; Branda, N. *Chem. Commun.* **1998**, 1257−1258.

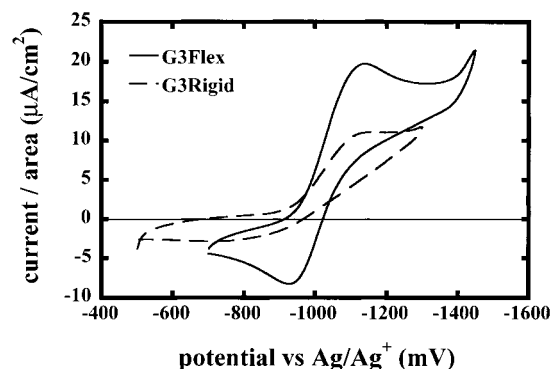(36) Pollak, K. W.; Sanford, E. M.; Fréchet, J. M. J. *J. Mater. Chem.* **1998**, *8*, 519−527.

(37) Nierengarten, J.-F.; Schall, C.; Nicoud, J.-F. *Angew. Chem., Int. Ed. Engl.* **1998**, *37*, 1934−1935.

(38) Kraus, G. A.; Louw, S. V. *J. Org. Chem.* **1998**, *63*, 7520−7521.

(39) Kimura, M.; Nakada, K.; Yamaguchi, Y.; Hanabusa, K.; Shirai, H.; Kobayashi, N. *Chem. Commun.* **1997**, 1215−1216.

(40) Brewis, M.; Clarkson, G. J.; Goddard, V.; Helliwell, M.; Holder, A. M.; McKeown, N. B. *Angew. Chem., Int. Ed. Engl.* **1998**, *37*, 1092−1094.

(41) Takada, K.; Díaz, D. J.; Abruña, H. D.; Cuadrado, I.; Casado, C.; Alonso, B.; Morán, M.; Losada, J. *J. Am. Chem. Soc.* **1997**, *119*, 10763−10773.

(42) Osteryoung, J.; O'Dea, J. J. In *Electroanalytical Chemistry: A Series of Advances*; Bard, A. J., Ed.; Marcel Dekker: New York, 1986; Vol. 14, pp 209−308.

(43) DePamphilis, B. V.; Averill, B. A.; Herskovitz, T.; Que, L., Jr.; Holm, R. H. *J. Am. Chem. Soc.* **1974**, *96*, 4159−4167.

(44) Que, L., Jr.; Anglin, J. R.; Bobrik, M. A.; Davison, A.; Holm, R. H. *J. Am. Chem. Soc.* **1974**, *96*, 6042−6048.

(45) Hill, C. L.; Renaud, J.; Holm, R. H.; Mortenson, L. E. *J. Am. Chem. Soc.* **1977**, *99*, 2549−2557.

Redox-Active Core Dendrimers

J. Am. Chem. Soc., Vol. 121, No. 43, 1999 9963
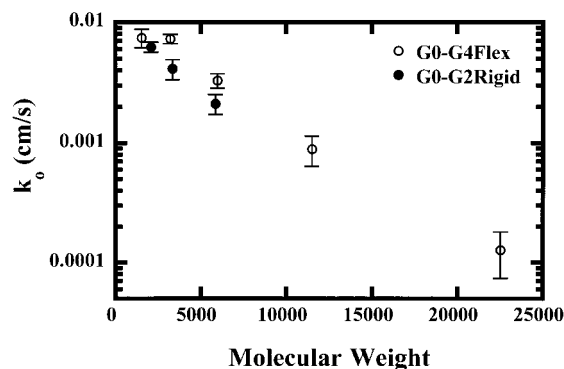
Figure 4. Electron-transfer rate attenuation as a function of molecular size and type.
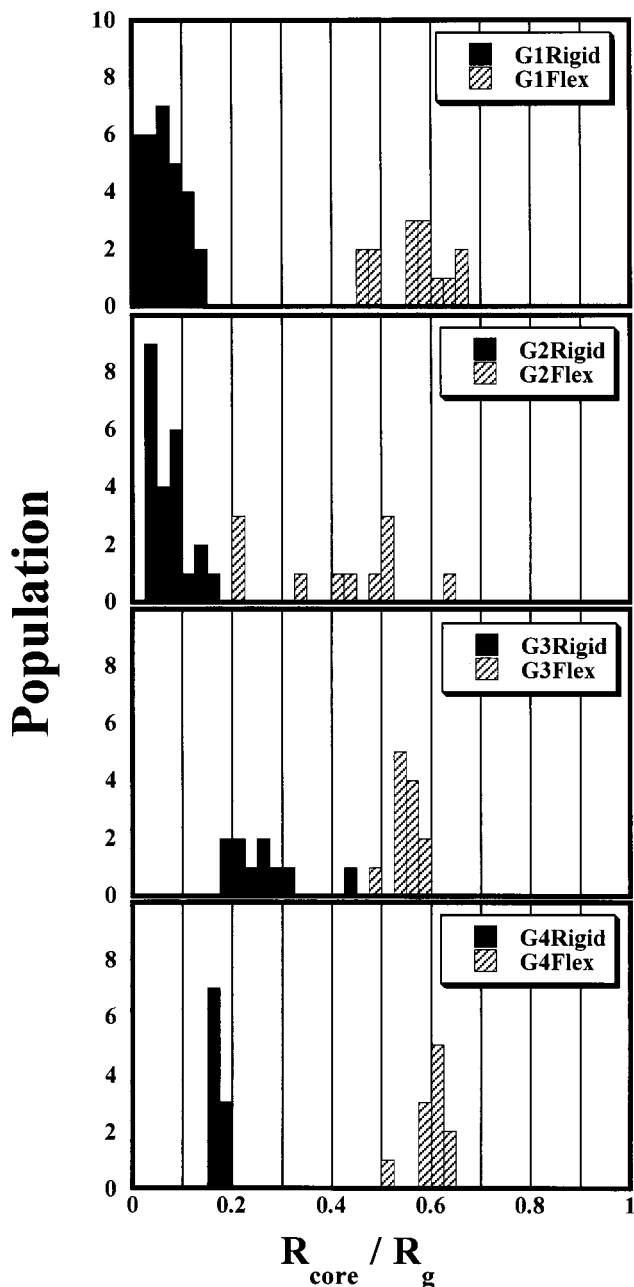
variance. Thus, it was of interest to generate models of the dendrimers in an effort to shed some light on structural differences in these molecules and to rationalize these differences in electron-transfer rate.

E. Illustration of Dendrimer Conformation with Molecular Structures Derived from Computational Conformational Searching. Dendrimers are conformationally complex and no structural data such as crystal structures are available that indicate minimum energy conformations for these molecules. Thus, the most important task in conducting a realistic simulation of dendrimer structure is finding the lowest energy minima in the potential space of such molecules. Thus, we turned to the technique of conformational searching in an attempt to generate a family of structures representative of the low-energy conformations of the dendrimers.[46-48]

Many details of this protocol are important. Such explications are provided in the Supporting Information. In performing these computations, we stress their correspondence with available experimental data and chemical intuition. Thus, one can regard these results as a proposed model of dendrimer conformation.

Our first interest in evaluating the results of these simulations was to determine the relative correlation between these results and available experimental data. In Table 1, the radii of gyration of the models obtained from these simulations are compared with the hydrodynamic radii obtained from NMR and electrochemistry experiments. A good correlation is expected if the model is reasonably spherical in shape and of the same size as the molecule (i.e., a noninteracting hard-sphere model). In the case of the flexible dendrimers, an excellent correlation between computationally determined radii of gyration and electrochemically determined hydrodynamic radii was found. This suggests that vacuum models can be reasonable approximations of the molecules investigated in DMF electrolyte solution. Poorer correlations were found for the flexible models with molecules in solution (particularly THF) suggesting solvent swelling in this solvent (Section C). A poor correlation was found between measured hydrodynamic radii and computed radii of gyration for the rigid molecules. This observation is not surprising given the open, nonspherical shape of the rigid molecules (see below). Unfortunately, there is no straightforward way to calculate a hydrodynamic radius from these models, so no further correlations can be made in this regard.

The most significant difference between flexible and rigid dendrimers is the relative position of the iron−sulfur core model in each type of dendrimer (Figure 5). The number of low-energy

(46) Sun, Y.; Kollman, P. A. *J. Comput. Chem.* **1992**, *13*, 33−40.
(47) O'Connor, S. D.; Smith, P. E.; Al-Obeidi, F.; Pettitt, B. M. *J. Med. Chem.* **1992**, *35*, 2870−2881.
(48) Al-Obeidi, F.; O'Connor, S. D.; Job, C.; Hruby, V. J.; Pettitt, B. M. *J. Peptide Res.* **1998**, *51*, 420−431.

Figure 5. Relative occurrence of conformers correlated with relative core offset. R_{core} refers to the distance between the center of the cubic core and the center of mass of the molecule. R_g refers to the radius of gyration of the molecular model. Bars in each histogram represent the number of structures found in a conformation search that were within a Boltzmann cutoff (10 kcal/mol) of the minimum energy structure found.
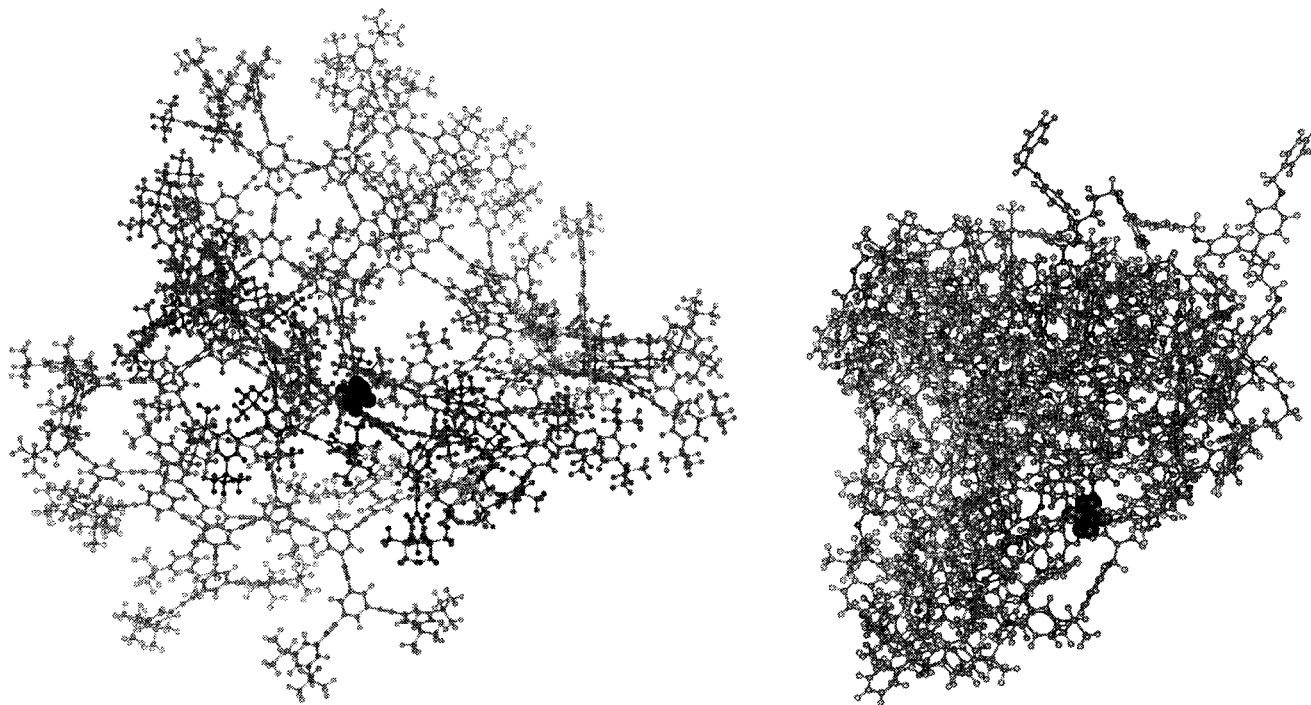
conformers (within a Boltzman cutoff of 10 kcal/mol at 500 K of the lowest energy conformer, see Supporting Information) was correlated with the relative offset of the core. An offset of zero would find the core at the center of mass of the molecule. An offset of one would find the core at the edge of the molecule. One can see a substantially more offset core in all of the flexible models compared with all of the rigid models. In pictorial representations of the lowest energy conformations of **G4Rigid** and **G4Flex** (Figure 6), the core is observed to be very centrally located in the rigid molecule but virtually at the molecular edge in the flexible molecule.

F. The Relationship between Molecular Structure and Electron-Transfer Rate Attenuation. Correlation of the results

Figure 6. Ball and stick models of the lowest energy conformations found for (left) **G4Rigid** and (right) **G4Flex** during the conformational search.

of these simulations with the electron-transfer rate data suggests the possibility that a component of electron transfer in the flexible dendrimers occurs on asymmetric conformers such as those shown in Figure 6. In contrast, in the stiff dendrimers, the redox core is held much more rigidly in the center of the molecule. This observation seems to rationalize the difference in relative electron-transfer rates between rigid and flexible dendrimers. The flexible dendrimers effectively encapsulate the molecular core less than the rigid dendrimers. Note that the open structure of the **G4Rigid** model in Figure 6 argues against the notion that access of the counterion to the redox unit is rate limiting.

Naturally, the electron-transfer rates measured experimentally here will represent some average over the orientations of the molecule with respect to the electrode and some average over the different conformations accessible to the molecules. Further discussion of each of these points is warranted. Is consideration of an orientational average important in rationalizing relative electron-transfer rates? Perhaps not. Murray et al. recently published results on the electrochemistry of ferrocene-terminated, 8-carbon alkanethiol-capped gold colloids of similar size to the molecules studied here.[49] A singular, multielectron redox wave was observed for ca. 15 surface-bound ferrocenes. The interpretation of this result was that the rotational motion of this particle was much faster than the time scale of the electrochemical experiment and thus the multiple, serial electron transfers appeared as one redox wave. This phenomenon plausibly would give rise to electrochemical behavior in our system that is also the result of rapid orientational averaging. Assuming a series of dendrimers in which the redox core is confined to a point at the molecular surface, the electron-transfer rate would vary, at most, as the relative surface area of the molecules (slow rotation limit) and, at least, would be invariant with molecular size (fast rotation limit). Clearly, the electron-transfer rate is attenuated more than this in the flexible dendrimers studied here. This result indicates that, although these

models help to paint a picture that distinguishes the flexible from the rigid dendrimers, they are static models, and that other dynamic behaviors are important here.

Significant changes in the core position within the flexible dendrimers probably occur on the time scale of the electrochemical experiment and are thus important to the encapsulation behavior as suggested by the range of minimum energy conformations illustrated in Figure 5. This trend persists for the other generations of molecules (see Supporting Information). The idea that the flexible dendrimers have a much more mobile core than do the rigid dendrimers is intuitive: the rigid dendrimers are plausibly much more shape persistent[29-31,50] and thus do not change shape nearly as much over time. Thus, they provide a system for encapsulation that is more ideal from both a static and a dynamic viewpoint.

Up until this point, it has been inferred that encapsulation is due to steric shielding of the redox couple from the electrode. The rigid dendrimers encapsulate the core better than the flexible dendrimers of a similar molecular weight as evidenced by attenuation of electron-transfer rates. This conclusion merely indicates that the rigid architectures separate the redox unit more efficiently from the electrode. However, one can also ask how the differing dendrimer units mediate electron transfer over comparable distances. Electron-transfer rate measurements on redox-active proteins[1-3] and the subsequent analysis of these rates with distance[4-7] suggests the dominance of a through-bond superexchange pathway for electron transfer. Distance dependence of electron-transfer rate, rather than being a measure of synthetic effort as was argued for molecular weight earlier, is interesting from the standpoint of understanding how units mediate electron transfer. In the case of these molecules, no truly accurate measure of distance is available. However, one might approximate core to perimeter distance using the results of the conformational searches presented. Using the radius of gyration as effectively an upper limit for the distance dependence

(49) Green, S. J.; Pietron, J. J.; Stokes, J. J.; Hostetler, M. J.; Vu, H.; Wuelfing, W. P.; Murray, R. W. *Langmuir* **1998**, *14*, 5612−5619.

(50) Pesak, D. J.; Moore, J. S. *Angew. Chem., Int. Ed. Engl.* **1997**, *36*, 1636−1639.
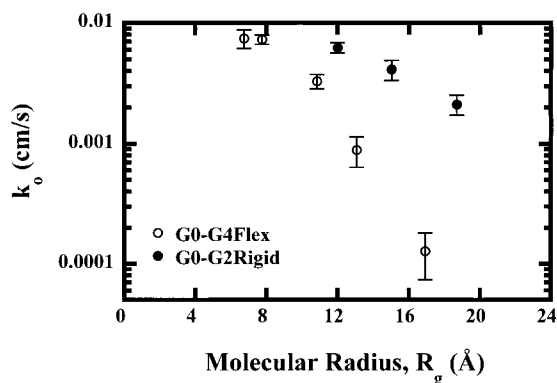
Figure 7. Distance dependence of electron-transfer rate using radius of gyration as an effective distance parameter.

of electron transfer, this relation was calculated. The results of this analysis are shown in Figure 7.

The most interesting conclusion of this figure is that rigid dendrimers pass electrons more efficiently than flexible dendrimers on a distance-weighted basis. This is in contrast to the relative behaviors of these series of molecules on a molecular weight-weighted basis. Phenyl acetylene linkages have been discussed as molecular wires previously.[51] It is noted that these architectures are cross conjugated (e.g., meta-linked) and that coupling of the donor and acceptor to the conjugated bridge may be more important parameters than the coupling within the conjugated bridge when determining electron-transfer rates.[52] However, despite these caveats, the phenyl acetylene architecture has higher energy filled and lower energy unfilled states and it requires passage of the electron through fewer bonds per unit distance than does the flexible architecture. Thus, we feel that finding this difference is not particularly unintuitive. Indeed, an effective β (the slope of $-\ln(k_0)$ versus distance) can be calculated as 0.16/Å for the rigid series and 0.40/Å for the flexible series. As these β values are computed from an approximated distance, they really cannot be compared with other values tabulated in the literature. Indeed, they are too small. One would expect a β for the rigid dendrimers closer to 0.57/Å (the value reported for electron transfer through phenyl acetylene units) and a β of 0.9/Å for the flexible dendrimers (the value reported for electron transfer through saturated units).[51] These differences suggest that the electron is being transferred over a distance shorter than that indicated by the radius of gyration of the molecule. This conclusion is somewhat obvious given the nonspherical but persistent shape of the rigid dendrimers and the asymmetric position of the core in the flexible dendrimers. However, these relative β values do illustrate an important difference between these two types of molecules and can serve to compare with other metallodendrimer electron-transfer studies that might be performed in the future.

Conclusions

Dendrimer structures can encapsulate electroactive centers and attenuate electron transfer to/from these centers. There exist real molecular structure—property relationships for this attenuation behavior as evidenced by the very different behaviors observed in flexible and rigid dendrimer structures. Although the flexible dendrimers do attenuate electron transfer, this

behavior does not arise from the type of steric shielding that one would expect if one considered the geometric structure of the dendrimer to resemble its topological structure. Rather, the results presented here suggest that the core is mobile within the structure of the flexible dendrimers, and its dynamics are probably the most important parameter in governing encapsulation in this series of molecules. In contrast, the rigid dendrimers are more shape persistent and represent architectures in which the electron-transfer rate attenuation is much more easily explained by steric shielding. Overall, the rigid series of dendrimers offers the better strategy for electron encapsulation on a molecular weight scale. When the distance dependence of electron transfer was approximated, however, the rigid dendrimers potentially may act as better mediators of electron transfer per unit distance. This statement is, however, tempered by uncertainties in geometry inherent in these molecules.

Experimental Section

Instrumentation for Routine Characterization. All syntheses that were air and/or moisture sensitive were performed either using standard Schlenk techniques under argon or in a nitrogen-filled Vacuum Atmospheres drybox. ^{1}H NMR were obtained with either a Gemini spectrometer operated at 300 MHz or a Varian spectrometer operating at 300 MHz. ^{13}C NMR spectra were obtained on a Gemini spectrometer operating at 75 MHz, or on a Varian spectrometer operating at 75 MHz. Chemical shifts were referenced to the chemical shifts of the residual protons of the NMR solvents.

MALDI-MS investigations were carried out using a Bruker Proflex+ (Bruker Daltonics, Billerica, MA) linear MALDI-TOF instrument with a 1.2 m flight tube. Further details are provided in the Supporting Information.

FAB-MS: A JEOL HX-110 (JEOL USA, Inc. Peabody, MA) sector instrument was used for analyzing the smaller generation dendrimers using FAB. The FAB gun was operated at 6−8 keV. The accelerating voltage was set at 10 keV. Samples were dissolved directly in the matrices, NBA or NPOE.

Electrospray-MS: A triple-quadrupole mass spectrometer, Micromass Quattro II (Micromass Inc., Beverly, MA), was used for analyzing the dendrimers using electrospray. Further details are provided in the Supporting Information.

Electrochemical Apparatus. Electrochemical experiments were carried out on a Bioanalytical Systems CV-50W Voltammetric Analyzer. The three-electrode cell consisted of a Pt disk working electrode with geometric area of 0.0201 cm^2, a Pt auxiliary electrode, and a homemade nonaqueous Ag/AgNO$_3$ reference electrode (Ag wire contacting a DMF solution of 0.01 M AgNO$_3$ and 0.1 M supporting electrolyte, tetraethylammonium tetrafluoroborate). All electrochemical experiments were carried out in a nitrogen-filled drybox at room temperature. Millimolar concentrations of the analytes were dissolved in DMF or 25% pyridine/75% DMF (v/v), which contained 0.1 M tetraethylammonium tetrafluoroborate (TEAF) supporting electrolyte.

Initially, Pt disk working electrodes were polished with 1 μm diamond paste (BAS) followed by 0.25 μm diamond suspension (BAS). Prior to each experiment, the Pt working electrode was cycled continuously at 100 mV/s in blank electrolyte solution to obtain the double layer capacitance response. If any faradaic signal was observed, the Pt disk was re-polished as indicated above.

The freshly prepared, homemade nonaqueous Ag/AgNO$_3$ reference electrode was calibrated against ferrocene before each experiment ($E_{1/2}$ = 32 mV for 4 mM in 0.1 M TEAF/DMF solution, average of 10 experiments) to provide a Fc/Fc$^+$ reference potential for each voltammetric experiment. The value of this reference was set to 32 mV vs this Fc/Fc$^+$ for all subsequent experiments. Ferrocene was not used as an internal reference to exclude the possibility of interacting with the macromolecular analyte.

Cyclic Voltammetry. Electron-transfer rate constants were calculated using the method of Nicholson[53] by using working curves that relate

(51) Sachs, S. B.; Dudek, S. P.; Hsung, R. P.; Sita, L. R.; Smalley, J. F.; Newton, M. D.; Feldberg, S. W.; Chidsey, C. E. D. *J. Am. Chem. Soc.* **1997**, *119*, 10563−10564 and references therein.

(52) Davis, W. B.; Svec, W. A.; Ratner, M. A.; Wasielewski, M. R. *Nature* **1998**, *396*, 60−63.

(53) Nicholson, R. S. *Anal. Chem.* **1965**, *37*, 1351−1354.

ΔE_p to the kinetic parameter Ψ. The rate constant was determined by the following equation:

$$k^o = \Psi\left[D_o\pi v\left(\frac{nF}{RT}\right)\right]^{1/2} \qquad (2)$$

where Ψ is the kinetic parameter related to ΔE_p, D_o is the diffusion coefficient (cm²/s), v is the potential sweep rate (V/s), n is the number of electrons passed, F is Faraday's constant, R is the gas constant, and T is the cell temperature. Potential sweep rates ranged from 25 to 500 mV/s for analytes displaying quasireversible electrochemical behavior at these scan rates. However, **G3Flex** displayed $\Delta E_p > 190$ mV at a sweep rate of 25 mV/s. Quasireversible kinetics were observable for this molecule only at very slow sweep rates (<3 mV/s).

Osteryoung Square Wave Voltammetry. Osteryoung square wave voltammetry[42,54,55] was performed using a step height of 4 mV, a sweep width amplitude of 25 mV, and a frequency of 15 Hz. Difference current was iteratively fit using FSQPLT software (provided by John J. O'Dea of the J. Osteryoung Group) to yield $E_{1/2}$, α, and $\log(\kappa/(t_d)^{1/2})$. Electron-transfer constant was calculated from the relation,

$$\log(\kappa(t_d)^{1/2}) = \log\frac{k_o}{D_o^{1/2}}t_d^{1/2} \qquad (3)$$

where t_d is the experimental pulse period, D_o is the molecular diffusion coefficient, and κ is the reduced rate constant.

Chronoamperometry. Chronoamperometry was carried out using a pulse width of 500 ms and a potential step height of 800 mV centered around $E_{1/2}$ for each molecule studied. Care was taken in choosing an experimental pulse width. Small pulse widths suffer from excess nonfaradaic current or non-steady-state cell conditions. Large pulse widths suffer from effects of convection and migration. A pulse width of 500 ms was chosen as this pulse width resided in the pulse-width independent region of the chronoamperometric diffusion–time plot. Linear portions of the Cottrell plots were iteratively fit using the Cottrell equation to yield the reported diffusion coefficient for each analyte.

Pulsed-Field-Gradient, Spin–Echo NMR. All experiments were carried out at 25 °C using a Bruker 500 MHz spectrometer (1996) with an Oxford narrow bore magnet (1989), SGI INDY host workstation, and XWINNMR software. The instrument was equipped with a three-channel gradient control unit (GRASPIII), variable-temperature unit, pre-cooling and temperature stabilization unit, and three frequency channels with waveform memory and amplitude shaping unit. A 5-mm i.d. ¹H/BB(¹⁰⁹Ag–³¹P) triple-axis gradient probe (ID500–5EB, Nalorac Cryogenic Corp.) was used for all ¹H diffusion measurements. The probe was equipped with actively shielded gradient coils. The gradient strength was calibrated using literature values for water diffusion in ¹H₂O/²H₂O mixtures. All samples were prepared in a nitrogen atmosphere in sealed NMR tubes.

The longitudinal eddy current (LED) pulse sequence was used in all PFGSE experiments.[56,57] The experimental data were collected by varying the pulse gradient ($g = 5$–53 G/cm over 16 increments) in the y-direction, and keeping the duration of the gradient pulse ($\delta = 5$

ms) and the pulse interval ($\Delta = 28$ ms) constant. The attenuation of signal intensities was tabulated by measuring the peak height at each pulse gradient. Stejskal–Tanner plots were generated. A nonlinear least-squares fitting procedure was carried out on the attenuation of signal intensities to evaluate the diffusion coefficient. Error in determining diffusion coefficients was primarily that in determining relative signal intensity, and error is reflected in Table 1.

Conformational Searching. Conformational searches were performed to generate a family of structures representative of the low-energy conformations of dendrimer models. Procedures similar to those reported previously were employed,[46–48] but with several differences that are detailed in the Supporting Information.

Synthesis. Tris(dibenzylideneacetone)dipalladium(chloroform),[58] $(Bu_4N)_2[Fe_4S_4(S\text{-}t\text{-}Bu)_4]$,[59] and S-Acetyl-4-iodophenol[60] were prepared as described in the literature. The flexible series of dendrimers were available from our preliminary study and are further characterized by ESI-MS and MALDI-MS-TOF as described below.

G0Flex. MALDI-TOF MS m/z calcd for $C_{68}H_{112}Fe_4\ N_6O_4S_8$ 1799 (M + nBu$_4$N), found 1798 (M + nBu$_4$N), dithranol matrix, positive ion mode. ESI-MS (m/z) 536.0 (M − 2 nBu$_4$N⁺, $z = 2$), negative ion mode.

G1Flex. MALDI-TOF MS m/z calcd for $C_{188}H_{224}Fe_4\ N_6O_{12}S_8$ 3483 (M + nBu$_4$N), found 3485 (M + nBu$_4$N), dithranol matrix, positive ion mode. ESI-MS (m/z) 1376.7 (M − 2 nBu$_4$N, $z = 2$), negative ion mode.

G2Flex. MALDI-TOF MS m/z calcd for $C_{380}H_{416}Fe_4\ N_6O_{28}S_8$ 6239 (M + nBu$_4$N), found 6242 (M + nBu$_4$N), dithranol matrix, positive ion mode. ESI-MS (m/z) 2754.4 (M − 2 nBu$_4$N, $z = 2$), negative ion mode.

G3Flex. MALDI-TOF MS m/z calcd for $C_{764}H_{800}Fe_4\ N_6O_{60}S_8$ 11022 (M + nBu$_4$N), found 11029 (M + nBu$_4$N), dithranol matrix, positive ion mode.

Rigid iron–sulfur cluster dendrimers are prepared as described in the Supporting Information.

Supporting Information Available: Cyclic voltammetry, chronoamperometry, and PFGSE data; details of the synthesis of rigid iron–sulfur core dendrimers; details of mass spectrometry; details and results of the conformational searching protocol employed (PDF). This material is available free of charge via the Internet at http://pubs.acs.org.

JA990875H

(54) O'Dea, J. J.; Osteryoung, J.; Osteryoung, R. A. *Anal. Chem.* **1981**, *53*, 695–701.

(55) Turner, J. A.; Christie, J. H.; Yukovic, M.; Osteryoung, R. A. *Anal. Chem.* **1977**, *49*, 1904–1908.

(56) Gibbs, S. J.; Johnson, C. S. *J. Magn. Reson.* **1991**, *93*, 395–402.

(57) Zeng, L.; Stejskal, E. O. *Appl. Spectrosc.* **1996**, *50*, 1402–1407.

(58) Ukai, T.; Kawajura, H.; Ishii, Y.; Bonnet, J. J.; Ibers, J. A. *J. Organomet. Chem.* **1974**, *65*, 253.

(59) Averill, B. A.; Herskovitz, T.; Holm, R. H.; Ibers, J. A. *J. Am. Chem. Soc.* **1973**, *95*, 3523–3534.

(60) Hsung, R. P.; Chidsey, C. E. D.; Sita, L. R. *Organometallics* **1995**, *14*, 4808–4815.